Anisotropic ferroelectric properties of anisotropically strained epitaxial NaNbO3 films

B. Cai, J. Schwarzkopf, E. Hollmann, M. Schmidbauer, M. O. Abdel-Hamed, and R. Wördenweber

Citation: Journal of Applied Physics **115**, 224103 (2014); doi: 10.1063/1.4882296
View online: http://dx.doi.org/10.1063/1.4882296
View Table of Contents: http://scitation.aip.org/content/aip/journal/jap/115/22?ver=pdfcov
Published by the AIP Publishing

Anisotropic ferroelectric properties of anisotropically strained epitaxial $NaNbO_3$ films

B. Cai,[1,a)] J. Schwarzkopf,[2] E. Hollmann,[1] M. Schmidbauer,[2] M. O. Abdel-Hamed,[1,3] and R. Wördenweber[1]
[1]*Peter Grünberg Institute (PGI) and JARA-Fundamentals of Future Information Technology, Forschungszentrum Jülich, D-52425 Jülich, Germany*
[2]*Leibniz Institute for Crystal Growth, Max-Born-Str. 2, D-12489 Berlin, Germany*
[3]*Faculty of Science, El-Minia University, Minia, Egypt*

(Received 13 March 2014; accepted 28 May 2014; published online 9 June 2014)

Epitaxial c-axis oriented $NaNbO_3$ films are grown on (110) oriented $NdGaO_3$ substrates. Due to the incorporated lattice strain the films show relaxor ferroelectric properties and an in-plane permittivity that is strongly enhanced with respect to unstrained $NaNbO_3$. Moreover, the lattice mismatch between substrate and film leads to an anisotropy in the compressive in-plain strain of -0.67% and -1.33% for the a- and b-direction of the films, respectively. As a consequence, the ferroelectric properties of the film depend strongly on the orientation of the applied electric field. The small anisotropy of the compressive in-plane strain leads to a large anisotropy of the permittivity, a shift of the peak in the temperature dependence of the permittivity, and different freezing temperatures and activation energies E_a of the relaxor ferroelectric film. © *2014 AIP Publishing LLC*.
[http://dx.doi.org/10.1063/1.4882296]

I. INTRODUCTION

Due to their ferroelectric and piezoelectric properties that are comparable to lead-zirconate-titanate (PZT)-based materials, alkali niobates have recently attracted significant scientific interest.[1–4] Among the family of alkali niobates, especially $NaNbO_3$ and $NaNbO_3$-based materials proved to be very promising candidates. Not only their complexity of phase transitions[2,4,5] and their highly interesting electric behavior[6] are of interest but also they represent promising candidates for lead-free and therefore eco-friendly thin film applications for instance in sensor and actuator devices.[1,7]

Generally, the physical properties of ferroelectric thin films can substantially differ from those in bulk materials. Especially, the two-dimensional "clamping" of a film onto a substrate with different lattice parameters can cause considerable strain of the film structure that may change profoundly the phase transition sequence, Curie temperature and permittivity in thin films with respect to that of unstrained bulk material.[8,9] Although recently the growth of $NaNbO_3$ on $SrRuO_3$ buffered $SrTiO_3$, MgO, or Rh substrates was reported,[10–13] the corresponding impact of epitaxial strain on the ferroelectric properties has not been studied in detail.

Recently, we have demonstrated that epitaxial $NaNbO_3$ films can be grown on various single crystalline oxide substrates ranging from $SrLaGaO_4$, $NdGaO_3$, $SrTiO_3$, $DyScO_3$, $TbScO_3$, to $GdScO_3$.[14] As a result of the lattice mismatch, the films are strained (tensile or compressive) and the ferroelectric properties are strongly modified.[6,15] In this paper, we focus on the impact of the anisotropy of the in-plane strain of epitaxially grown $NaNbO_3$ on (110)$NdGaO_3$. We demonstrate that this anisotropy leads to a large anisotropy in all ferroelectric properties ranging from the permittivity, Curie temperature, to the relaxor properties.

II. EXPERIMENTAL TECHNIQUES AND SAMPLE PREPARATION

$NaNbO_3$ films are deposited via liquid delivery spin metal organic chemical vapor deposition (MOCVD) at a temperature of 700 °C onto (110) oriented single crystalline $NdGaO_3$ substrates. The $NdGaO_3$ substrates are slightly off-oriented (0.1°) and annealed in pure oxygen flow at 1050 °C. This generates a regular step-and-terrace surface structure with NdO surface termination[16] and promotes step flow growth of the $NaNbO_3$ film. A detailed description of the MOCVD deposition technique is given in Ref. 14. At room temperature, the crystal structure of the substrate $NdGaO_3$ is orthorhombic ($a_{NGO} = 0.5428$ nm, $b_{NGO} = 0.5498$ nm, $c_{NGO} = 0.7709$ nm[17]) and the (110) surface exhibits a nearly squared in-plane lattice with lattice parameters 2×0.3855 nm and 2×0.3863 nm in [001] and [1$\underline{1}$0] direction, respectively. Onto this square in-plane lattice the $NaNbO_3$ film is deposited. At room temperature, the orthorhombic unit cell lattice parameters of bulk $NaNbO_3$ are $a_{NNO} = 0.55047$ nm, $b_{NNO} = 0.55687$ nm, and $c_{NNO} = 1.5523$ nm, respectively.[18] For simplicity, $NaNbO_3$ is often presented in pseudocubic notation with the corresponding pseudocubic lattice parameters $a^{pc}{}_{NNO} = 0.3881$ nm and $b^{pc}{}_{NNO} = c^{pc}{}_{NNO} = 0.3915$ nm.[19] Due to energy minimization, $NaNbO_3$ is expected to grow with the smallest possible distortion on $NdGaO_3$ which is achieved by the c^{pc}-orientation of the $NaNbO_3$ film. The resulting lattice mismatch $\beta = (2a_{film} - a_{sub})/a_{sub}$ in a^{pc}- and b^{pc}-direction is compressive and highly anisotropic, i.e., ~0.67% and ~1.35%, respectively. Here, a_{film} and a_{sub} represent the pseudocubic lattice parameters in a^{pc} or b^{pc} direction of the film and the corresponding effective in-plane lattice dimensions in [001] or [1$\underline{1}$0] direction of the substrate.

a)Author to whom correspondence should be addressed. Electronic mail: b.cai@fz-juelich.de

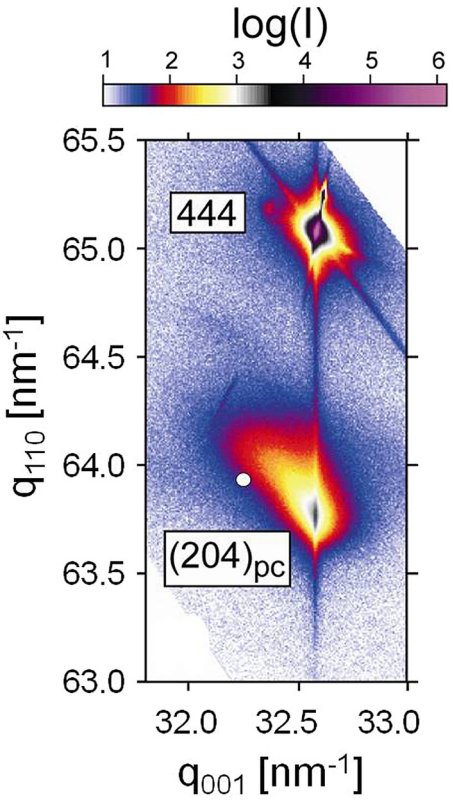

FIG. 1. RSM in the vicinity of the (444) Bragg reflection of the $NdGaO_3$ substrate. The circle marks the position of the corresponding (204) reflex of unstrained bulk $NaNbO_3$.

The structural properties of the $NaNbO_3$ films are analyzed via high resolution X-ray diffraction experiments.[14] Reciprocal space maps (RSMs) in the vicinity of the asymmetric (444) and (260) Bragg reflections of the $NdGaO_3$ substrate (exemplarily shown for the (444) Bragg reflection on an 80 nm thick $NaNbO_3$ film in Fig. 1) reveal epitaxial growth of the film. Although they indicate the onset of partial plastic relaxation of the incorporated compressive strain for the films with a film thickness larger than ~15 nm toward the lattice parameters of bulk $NaNbO_3$ (see the mark in Fig. 1), the in-plane components of the main scattering vectors of the film peaks are identical to those of the (444) and (260) Bragg reflections of the $NdGaO_3$ substrate. The resulting lattice parameters and epitaxial relationships are given in Table I. Note that the surface normal and in-plane directions of the $NdGaO_3$ substrate and the $NaNbO_3$ film refer to the orthorhombic and pseudocubic notation, respectively. Furthermore, the resulting strain $\eta = (a_{film} - a_{nom})/a_{nom}$ is compressive in a^{pc}- and b^{pc}-direction (−0.67% and −1.33%) and tensile in c^{pc}-direction (0.77%). Here, a_{film} and a_{nom} represent the experimentally determined lattice parameter and the lattice parameter of unstrained $NaNbO_3$, respectively. Owing to the Poisson effect, the compressive in-plane strain will automatically result in a tensile strain in c^{pc}-direction. We estimated the Poisson's ratio to be $\nu \approx 0.52$ in our system, which agrees with the expectation for compressible materials of $\nu \approx 0.5$ and literature values of $\nu = 0.32$–0.36 obtained for various oxides.[20] From the small vertical splitting of the $(024)_{pc}$ Bragg reflection (similar to that we have observed in Ref. 14), we conclude to a slightly monoclinically distorted unit cell which is obtained by a shearing of the pseudocubic unit cell in $[110]^{pc}$ direction.[21,22]

For the investigation of the in-plane dielectric properties of the $NaNbO_3$ films, planar capacitors based on interdigitated electrodes (IDE) are employed. The IDEs are prepared via lift-off lithography technique and deposition of a thin (50 nm) Au layer. In order to obtain a reliable and large signal, a relatively large gap size $s = 5\ \mu$m is chosen that is compensated by large length $d = 700\ \mu$m of the individual IDE's fingers (width of the finger is 10 μm) and a large number (64) of fingers resulting in an effective length of the capacitor of 44.1 mm.[23] In order to avoid stray fields, the gap is strongly extended at the end of each finger (45 μm). This guarantees that the electric field E is oriented perpendicular to the direction of the fingers. Three different orientations of the IDE are prepared on each sample, which allow to determine the ferroelectric properties for electric field E with orientations along the longer axis ($E \| [110]NdGaO_3 \| [010]NaNbO_3$), the short axis ($E \| [001]NdGa\bar{O}_3 \| [100]NaNbO_3$), and diagonal ($E \| [1\bar{1}1]NdGaO_3 \| [110]NaNbO_3$), respectively. In the following, the orientation is denoted by the orientation α of the electric field with respect to the shorter axis (see sketch Fig. 2(a)).

The ferroelectric properties are analyzed in cryoelectric experiments (20 K–320 K) as function of frequency (20 Hz–2 MHz) and dc-bias voltage (−30 V–30 V) using a high precision capacitance meter (HP4278A) and a LCR meter (ST2826A). The in-plane real part of the dielectric constant ε' of the $NaNbO_3$ films is calculated using a *partial capacitance model*.[24–26] The model is based on conformal mapping and allows to evaluate the capacitive contribution of all components (esp., substrate and ferroelectric film) of planar structures. The model of Gevorgian *et al.*[25] is strictly valid for our geometry. However, due to the geometrical design of the IDE and the large permittivity of the $NaNbO_3$ films in

TABLE I. Lattice parameters, lattice mismatch, and experimentally determined strain for epitaxial grown $NaNbO_3$ on $NdGaO_3$.

Direction			Lattice parameter (nm)				
	$NdGaO_3$	$NaNbO_3$	$NdGaO_3$[a]	$NaNbO_3$[a]	$NaNbO_3$[b]	Lattice mismatch β (%)	Strain η (%)
In-plane	[001]	$[100]^{pc}$	2 × 0.3855 (Ref. 17)	0.3855	0.3881 (Ref. 19)	0.67	−0.67
	$[1\bar{1}0]$	$[010]^{pc}$	2 × 0.3863 (Ref. 17)	0.3863	0.3915 (Ref. 19)	1.35	−1.33
Out-of-plane	[110]	$[001]^{pc}$		0.3945	0.3915 (Ref. 19)		0.77

[a]Experimental values.
[b]Literature data.

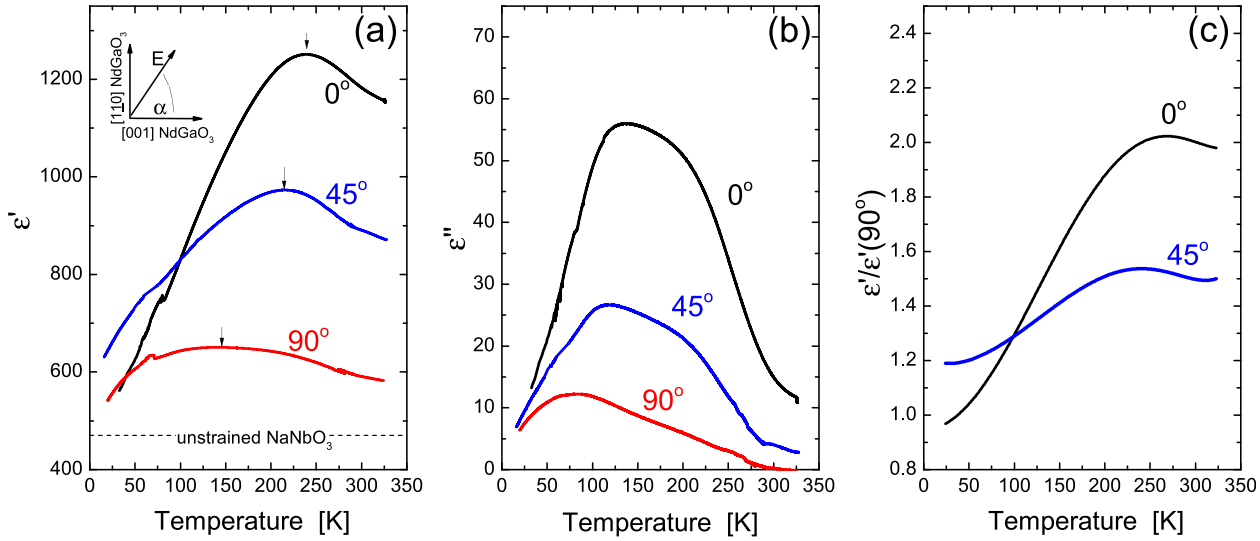

FIG. 2. Temperature dependence of the real (a) and imaginary (b) part of the dielectric constant for an 80 nm thick $NaNbO_3$ film on (110) $NdGaO_3$ measured at 1 MHz for different directions α of the electric field vector E. Additionally, the anisotropy of the permittivity for electric fields in the different crystallographic directions is given in (c). The angle α defines the orientation of the electric field direction with respect to the shorter crystallographic axis of film and substrate, i.e., for 0° the electric field E is oriented along [001] $NdGaO_3$||[100]^{pc} $NaNbO_3$ (see sketch in (a)). The dashed line in (a) marks typical value for the permittivity of unstrained bulk $NaNbO_3$.[27]

comparison to that of the substrate, all three models yield nearly identical results. The model proposed by Vendik[24] is employed in this paper. The imaginary part of the dielectric constant is obtained from the loss tangent $\tan\delta = \varepsilon''/\varepsilon'$ of the layer which is corrected for the contribution of the $NdGaO_3$ substrate. Part of the results measured for the direction of the electric field along the [100] $NaNbO_3$ (lowest strain) have been reported in Ref. 6.

III. EXPERIMENTAL RESULTS AND DISCUSSION

Fig. 2 shows the dielectric properties of an 80 nm thick $NaNbO_3$ film on (110) $NdGaO_3$ for different orientations of the electric field vector E. For all orientations and the complete temperature range, the in-plane permittivity of the strained film is considerably larger than the typical permittivity reported for unstrained $NaNbO_3$ bulk material ($\varepsilon' < 500$ for $T < 350$ K (Ref. 27)). Moreover, in all cases a distinct maximum is observed at T_{max} in the ε'-vs.-T dependence. However, the maximum of the permittivity and its position strongly depend on the orientation of the applied field. For E oriented along the direction of the lowest strain ($\alpha = 0°$) permittivity and T_{max} are largest, whereas for the orientation of E along the direction of strongest strain ($\alpha = 90°$), the smallest values are obtained for permittivity and T_{max}. The maxima are $\varepsilon'_{max} = 1296$ at $T_{max} = 249$ K, $\varepsilon'_{max} = 973$ at $T_{max} = 216$ K, and $\varepsilon'_{max} = 649$ at $T_{max} = 121$ K for the orientations 0°, 45°, and 90°, respectively. The anisotropy of the permittivity is quite large. Values up to $\varepsilon'(0°)/\ \varepsilon'(90°) \approx 2$ are obtained at room temperature (see Fig. 2(c)). Generally, a peak in the temperature dependence of the permittivity is an indication of a transition of the ferroelectric state which will be discussed in the following below. However, for all orientations the peak is rather broad with the tendency of broader peaks for E oriented along the larger strain.

It is known that substrate-induced biaxial strain may significantly increase the spontaneous polarization and induce structural and, therefore, ferroelectric phase transitions in a ferroelectric material.[8,9,28] These effects not only depend on the amount of strain but also they are strongly affected by the sign of the strain (compressive or tensile) and the electric field direction in which the polarization is measured. For example, it has been shown that tensile strain significantly increases T_c for in-plane polarization measurements on $SrTiO_3$ films, whereas compressive strain does not induce any spontaneous in-plane polarization in the same material.[8,9] In order to examine the ferroelectric state of the strained film dc bias dependent measurements were performed.

Fig. 3 shows examples of the dc electric field dependence of the strained $NaNbO_3$ film for different temperatures and field orientations. The dc bias is oriented parallel to the ac field of the measurement. In all cases, a butterfly shape is observed indicating the presence of spontaneous polarization and tunability. Spontaneous polarization has also been recorded by piezo force microscopy and Sawyer-Tower measurements at room temperature. Nevertheless, they cannot be excluded, that the butterfly shape is also partially caused by motions of domain walls.[29] At room temperature, the tunability and spontaneous polarization (and possibly domain wall motions) are largest for the 0° orientation (smallest strain).

More details of the ferroelectric properties of the sample can be obtained by the analysis of the hysteretic behavior of the bias dependence of the permittivity. Fig. 4 shows $\Delta\varepsilon' = \varepsilon'(\text{increasing bias}) - \varepsilon'(\text{decreasing bias})$ for the E orientation $\alpha = 0°$ that yields the largest tunability and hysteresis at room temperature. For all measured temperatures, the presence of a spontaneous polarization is indicated and a maximum $\Delta\varepsilon'_{max}$ is visible at an electric fields E_{max} that coincides with the coercive voltage of the ferroelectric film.[30] The temperature dependence of E_{max} (inset of Fig. 4(a)) as well as the decrease of $\Delta\varepsilon'_{max}$ above room temperature indicate that the

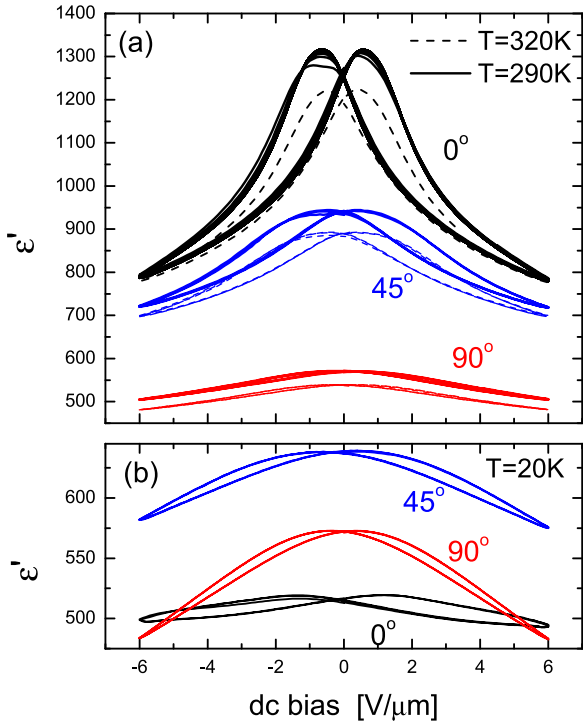

FIG. 3. Electric field dependence of the permittivity of the 80 nm thick $NaNbO_3$ on (110) $NdGaO_3$ measured at 1 MHz for different orientations α of the electric field E and different temperatures 320 K (dashed lines in (a)), 290 K (solid lines in (a)), and 20 K (b).

ferroelectric state will most likely disappear at higher temperatures. The linear decrease of E_{max}–vs.-T (inset of Fig. 4(a)) hints at a transition temperature close to 400 K. Unfortunately, this temperature cannot be established in our experimental setup.

A closer look at the dc-bias dependence of $\Delta\varepsilon'$ (Fig. 4(b)) around zero bias reveals more details of the ferroelectric properties of the strained film. At high temperatures ($T > 270$ K), $\Delta\varepsilon'$ shows the classic ferroelectric behavior, i.e., a linear increase around zero bias. However, at lower temperature the bias dependence shows an "S" shape which is indicative for antiferroelectric behavior or antiferroelectric contributions. In particular, the data recorded at 260 K show a clear plateau at zero bias, i.e., the film behaves antiferroelectric. At lower temperatures, the plateau inclines, i.e., there seems to be antiferroelectric and ferroelectric behavior in the sample. Finally, at the lowest temperatures ($T < 100$ K, see Fig. 4(a)) the dependence is again linear. Either the antiferroelectric contribution has vanished or it is too small to be detected in our measurement. Strained $NaNbO_3$ is known to be a relaxor-type ferroelectric.[6] The transition from ferro- to antiferroelectric behavior at temperatures around 270 K might be connected to properties of polar regions of the relaxor ferroelectric state of the sample which is discussed below. Another possible interpretation of the plateau in the dc-bias dependence of $\Delta\varepsilon'$ is given by pinning of domain walls.[31] However, it is questionable why this effect vanishes at lower temperature where the pinning increases.

Relaxor ferroelectrics or relaxors represent a class of disordered ferroelectric crystals with particular structure and properties.[32] At high temperature, they exist in a non-polar paraelectric phase that is similar in many respects to the paraelectric phase of classical ferroelectrics. Upon cooling, they transform into the ergodic relaxor state which is caused by polar nanoregions (PNR) with randomly distributed directions of electric dipoles. In principle, this transformation is not considered to be a structural phase transition since it is not accompanied by any change of crystal structure on macroscopic or mesoscopic scale. Nevertheless, the PNRs strongly affect the ferroelectric properties of the crystalline material and the state is often considered to be a new phase, the *relaxor ferroelectric phase*.

Due to the small, temperature dependent mobility of the PNRs, characteristic features should be observed in frequency dependent measurements of the ferroelectric properties in the relaxor regime. Especially, at the transition to the relaxor ferroelectric state the permittivity and the maximum in the ε'-vs.-T characteristic are expected to be frequency dependent. Fig. 5(a) shows the temperature dependence of the permittivity for different frequencies. Especially at the peak in ε' large differences in the permittivity are recorded for different frequencies. With increasing frequency the permittivity decreases and the temperature of the maximum permittivity

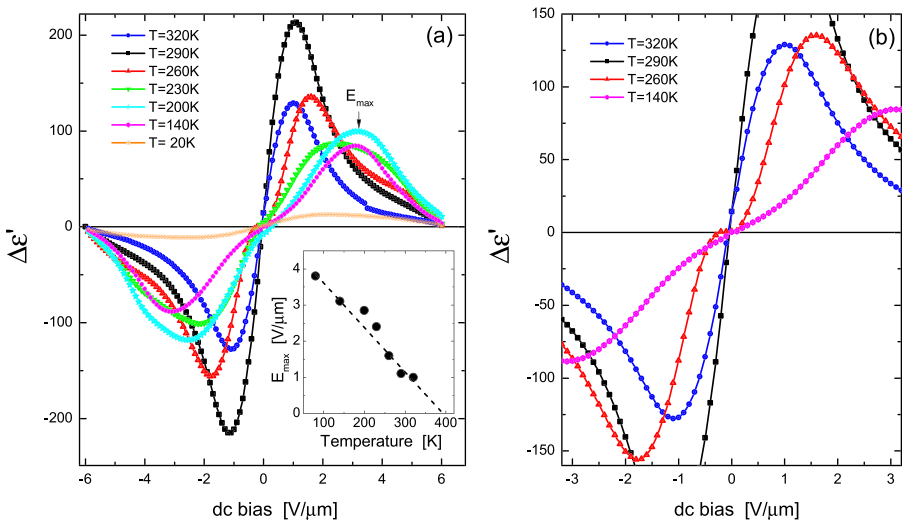

FIG. 4. Electric field dependence of the hysteretic behavior of the permittivity $\Delta\varepsilon' = \varepsilon'$(increasing bias) $- \varepsilon'$(decreasing bias) of the 80 nm thick $NaNbO_3$ film on (110) $NdGaO_3$ measured at 1 MHz for $\alpha = 0°$. The inset in (a) represents the temperature dependence of the position of the maxima as indicated by an arrow for one temperature in (a), (b) represents an enlarged plot of the bias dependence of $\Delta\varepsilon'$ around zero bias for selected temperatures.

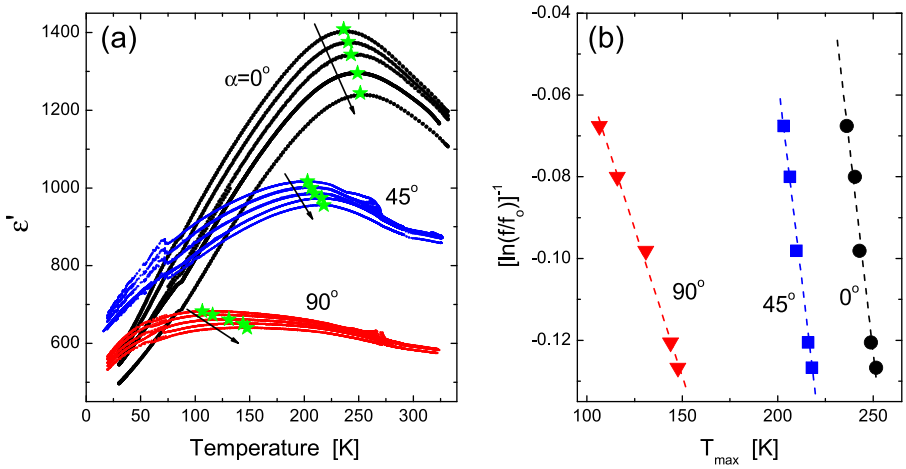

FIG. 5. (a) Permittivity as function of the temperature for different frequencies (1.5kHz, 15 kHz, 150 kHz, 1 MHz, and 1.5 MHz, the direction of increasing frequency is indicated by the arrows) and the different field orientations, the maxima positions T_{max} are marked by symbols, and (b) the resulting *Vogel-Fulcher* fits (dotted lines) based on Eq. (1) and an attempt frequency $f_o = 4$ GHz for the different electric field orientations.

T_{max} increases. This behavior is characteristic for many relaxor ferroelectrics,[33,34] it is described by the Vogel-Fulcher equation[35]

$$f = (2\pi\tau_o)^{-1} \exp\left[-\frac{E_a}{k_B(T_{\max} - T_{VF})}\right], \qquad (1)$$

with the attempt frequency $f_o = (2\pi\tau_o)^{-1}$, the activation energy E_a, Boltzmann constant k_B, and the static freezing temperature T_{VF}.

A *Vogel-Fulcher equation fit* of our permittivity data measured for frequencies ranging between 1.5 kHz and 1.5 MHz is given in Fig. 5(b). It demonstrates the predicted linear relation between the reduced frequency $[\ln(f/f_o)]^{-1}$ and T_{max}. Inserting a reasonable value $f_o = 4$ GHz for the attempt frequency yields, the static freezing temperature T_{VF} and the activation energy E_a. Values of $T_{VF} = 219.7$ K and $E_a = 21.2$ meV, $T_{VF} = 187.8$ K and $E_a = 21.5$ meV, and $T_{VF} = 61.4$ K and $E_a = 61.6$ meV are obtained for 0°, 45°, and 90° oriented IDEs, respectively. The values obtained for E_a are comparable to values reported for activation energies of a relaxor ferroelectric in the literature.[33,36] It should be noted that an increase of the compressive strain by a factor of about 2 reduces the freezing temperature by ~150 K and enhances the activation energy by a factor of about 3.

IV. CONCLUSION

We have demonstrated that the lattice mismatch between (110) oriented $NdGaO_3$ substrates and $NaNbO_3$ films leads to significant and anisotropic modifications of structural and ferroelectric properties of the $NaNbO_3$ films. Generally, the in-plane permittivity of the strained film is strongly enhanced as compared to bulk $NaNbO_3$ and shows relaxor type behavior. The small anisotropy of the compressive in-plane strain in the c-oriented $NaNbO_3$ film of −0.67% and −1.33% for the a^{pc}- and b^{pc}-direction, respectively, leads to a significant anisotropy of the ferroelectric properties: (i) a large anisotropy of the permittivity $(\varepsilon'(\alpha = 0°)/\varepsilon'(\alpha = 90°) \approx 2$ at room temperature), (ii) the maxima in the permittivity-vs.-temperature plots depend on the orientation of the electric field ($T_{max}(\alpha = 0°) = 249$ K and $T_{max}(\alpha = 90°) = 121$ K), and (iii) the relaxor properties expressed by the freezing temperature T_{VF} and the activation energy E_a differ strongly for different orientations of the electric field. Furthermore, dc-bias dependent measurements of the permittivity seem to reveal a transition from ferro- to antiferroelectric behavior at about 270 K. The antiferroelectric state vanishes or cannot be detected anymore at low temperature. In summary, anisotropically strained $NaNbO_3$ represents an ideal and extremely complex candidate for the examination of "strain engineering" of structural and ferroelectric properties of thin ferroelectric films.

ACKNOWLEDGMENTS

The authors would like to thank A. Offenhäusser, R. Kutzner, T. Grellmann, K. Greben, A. Markov, and S. Markschies for their valuable support. Financial support from China Scholarship Council (CSC) is also gratefully acknowledged.

[1]Y. Saito, H. Takao, T. Tani, T. Nonoyama, K. Takatori, T. Homma, T. Nagaya, and M. Nakamura, Nature **432**, 84 (2004).
[2]Y. I. Yuzyuk, R. A. Shakhovoy, S. I. Raevskaya, I. P. Raevski, M. El Marssi, M. G. Karkut, and P. Simon, Appl. Phys. Lett. **96**, 222904 (2010).
[3]V. Lingwal and N. S. Panwar, J. Appl. Phys. **94**, 4571 (2003).
[4]S. K. Mishra, N. Choudhury, S. L. Chaplot, P. S. R. Krishna, and R. Mittal, Phys. Rev. B **76**, 024110 (2007).
[5]H. D. Megaw, Ferroelectrics **7**, 87 (1974).
[6]R. Wördenweber, J. Schwarzkopf, E. Hollmann, A. Duk, B. Cai, and M. Schmidbauer, Appl. Phys. Lett. **103**, 132908 (2013).
[7]E. Cross, Nature **432**, 24 (2004).
[8]J. H. Haeni, P. Irvin, W. Chang, R. Uecker, P. Reiche, Y. L. Li, S. Choudhury, W. Tian, M. E. Hawley, B. Craigo, A. K. Tagantsev, X. Q. Pan, S. K. Streiffer, L. Q. Chen, S. W. Kirchoefer, J. Levy, and D. G. Schlom, Nature **430**, 758 (2004).
[9]R. Wördenweber, E. Hollmann, R. Kutzner, and J. Schubert, J. Appl. Phys. **102**, 044119 (2007).
[10]T. Saito, H. Adachi, T. Wada, and H. Adachi, Jpn. J. Appl. Phys., Part 1 **44**, 6969 (2005).
[11]T. Mino, S. Kuwajima, T. Suzuki, I. Kanno, H. Kotera, and K. Wasa, Jpn. J. Appl. Phys., Part 1 **46**, 6960 (2007).
[12]W. J. Maeng, I. Jung, and J. Y. Son, J. Cryst. Growth **349**, 24 (2012).
[13]S. Yamazoe, A. Kohori, H. Sakurai, Y. Kitanaka, Y. Noguchi, M. Miyayama, and T. Wada, J. Appl. Phys. **112**, 052007 (2012).
[14]J. Schwarzkopf, M. Schmidbauer, T. Remmele, A. Duk, A. Kwasniewski, S. Bin Anooz, A. Devi, and R. Fornari, J. Appl. Crystallogr. **45**, 1015 (2012).
[15]A. Duk, M. Schmidbauer, and J. Schwarzkopf, Appl. Phys. Lett. **102**, 091903 (2013).

[16]R. Dirsyte, J. Schwarzkopf, G. Wagner, J. Lienemann, M. Busch, H. Winter, and R. Fornari, Appl. Surf. Sci. **255**, 8685–8687 (2009).
[17]M. Schmidbauer, A. Kwasniewski, and J. Schwarzkopf, Acta Cryst. B **68**, 8–14 (2012).
[18]M. C. Morris, H. F. McMurdie, E. H. Evans, B. Paretzkin, H. S. Parker, N. C. Panagiotopoulos, and C. R. Hubbard, "Standard X-ray Diffraction Powder Patterns," Natl. Bur. Stand. (U.S.) Monograph No. 18, National Bureau of Standards, Gaithersburg, 1981.
[19]A. Vailionis, H. Boschker, W. Siemons, E. P. Houwman, D. H. A. Blank, G. Rijnders, and G. Koster, Phys. Rev. B **83**, 064101 (2011).
[20]A. Selçuk and A. Atkinson, J. Eur. Ceram. Soc. **17**, 1523 (1997).
[21]H. M. Christen, J. H. Nam, H. S. Kim, A. J. Hatt, and N. A. Spaldin, Phys. Rev. B **83**, 144107 (2011).
[22]Z. Chen, Z. Luo, C. Huang, Y. Qi, P. Yang, L. You, C. Hu, T. Wu, J. Wang, C. Gao, T. Sritharan, and L. Chen, Adv. Funct. Mater. **21**, 133 (2011).
[23]R. Wördenweber, J. Schubert, T. Ehlig, and E. Hollmann, J. Appl. Phys. **113**, 164103 (2013).
[24]O. G. Vendik, S. P. Zubko, and M. A. Nikol'skii, Tech. Phys. **44**, 349–355 (1999); O. G. Vendik and M. A. Nikol'skii, *ibid.* **46**, 112–116 (2001).
[25]S. S. Gevorgian, T. Martinsson, P. L. Linner, and E. L. Kollberg, IEEE Trans. Microwave Theory Tech. **44**, 896 (1996).
[26]E. Chen and S. Y. Chou, IEEE Trans. Microwave Theory Tech. **45**, 939 (1997).
[27]G. Shirane, R. Newnham, and R. Pepinsky, Phys. Rev. **96**, 581–588 (1954).
[28]N. A. Pertsev, A. G. Zembilgotov, and A. K. Tagantsev, Phys. Rev. Lett. **80**, 1988 (1998); N. A. Pertsev, V. G. Kukhar, H. Kohlstedt, and R. Waser, Phys. Rev. B **67**, 054107 (2003).
[29]D. Bolten, O. Lohse, M. Grossmann, and R. Waser, Ferroelectrics **221**, 251 (1999).
[30]O. Lohse, M. Grossmann, U. Boettger, D. Bolten, and R. Waser, J. Appl. Phys. **89**, 2332 (2001).
[31]D. V. Taylor and D. Damjanovic, J. Appl. Phys. **82**, 1973 (1997).
[32]A. A. Bokov and Z.-G. Ye, Solid State Commun. **116**, 105 (2000).
[33]D. Viehland, S. J. Jang, L. E. Cross, and M. Wuttig, J. Appl. Phys. **68**, 2916 (1990).
[34]A. A. Bokov and Z.-G. Ye, J. Mater. Sci. **41**, 31–52 (2006).
[35]H. Vogel, Phys. Z. **22**, 645 (1921); G. S. Fulcher, J. Am. Ceram. Soc. **8**, 339 (1925).
[36]H. W. Jang, A. Kumar, S. Denev, M. D. Biegalski, P. Maksymovych, C. W. Bark, C. T. Nelson, C. M. Folkman, S. H. Baek, N. Balke, C. M. Brooks, D. A. Tenne, D. G. Schlom, L. Q. Chen, X. Q. Pan, S. V. Kalinin, V. Gopalan, and C. B. Eom, Phys. Rev. Lett. **104**, 197601 (2010).